JOURNAL OF MATERIALS SCIENCE 26 (1991) 4727–4732

Sintering chemical reactions to increase thermal conductivity of aluminium nitride

KOJI WATARI, MITSURU KAWAMOTO, KOZO ISHIZAKI
Department of Materials Science and Engineering, School of Mechanical Engineering, Nagaoka University of Technology, Nagaoka, 940-21, Japan

Chemical reactions to increase thermal conductivity by decreasing oxygen contents during AlN sintering with an Y_2O_3 additive in a reducing nitrogen atmosphere with carbon were investigated. They were: $Al_2O_3 + N_2 + 3CO \leftrightharpoons 2AlN + 3CO_2$, $Al_2Y_4O_9 + N_2 + 3CO \leftrightharpoons 2AlN + 2Y_2O_3 + 3CO_2$ and $Y_2O_3 + N_2 + 3CO \leftrightharpoons 2YN + 3CO_2$. Some of the CO_2 gas reduced to CO gas in the presence of carbon by a chemical reaction: $CO_2 + C \leftrightharpoons 2CO$. These reactions were confirmed by examining oxygen contents, the grain boundary phases of the sintered AlN, and the trapped CO and CO_2 gases in the sintered bodies. These reducing reactions proceed with increasing sintering temperature and periods, and hence the thermal conductivity is increased.

1. Introduction

Aluminium nitride (AlN) ceramic has been considered as the future substrate material of electronic package. It is, however, difficult to obtain fully densified AlN ceramic [1]. Also AlN thermal conductivity is decreased by the presence of oxygen impurity [2–4]. Slack reported that oxygen, dissolved in the AlN lattice, creates aluminum vacancies which scatter phonons and that the thermal conductivity decreases as the oxygen content increases [2]. Sakai *et al.* reported that oxygen atoms form an oxynitride spinel phase and/or an AlN pseudo-polytype phase in the grain boundaries of sintered AlN without additives, which reduce the thermal conductivity greatly [3].

Recently, some usefully additives such as Y_2O_3, CaO, CaC_2 and $Ca(NO_3)_2$, have been reported for the fabrication of fully densified and highly thermally conductive AlN [4–9]. Y_2O_3 improves the thermal conductivity better than other additives [9]. It is considered that the addition of Y_2O_3 causes the precipitation of Y–Al–O compounds such as $YAlO_3$ and $Al_2Y_4O_9$ ($2Y_2O_3 \cdot Al_2O_3$) in the grain boundaries and then lowers the oxygen content dissolved in AlN grains [9].

On the other hand, more highly thermally conductive AlN ($> 230\ Wm^{-1}K^{-1}$) can be obtained by sintering in a reducing atmosphere, with higher sintering temperatures and longer sintering periods [10–12]. However, the chemical reactions to improve the thermal conductivity under reducing atmosphere have not been well studied.

In this work, chemical reactions to increase thermal conductivity by decreasing the oxygen content during AlN sintering using a Y_2O_3 additive and a reducing nitrogen atmosphere with carbon were clarified from experimental results.

2. Experimental procedure

A commercial AlN powder (Tokuyama Soda) with an average particle size of 0.6 μm and a specific surface area of $3.2\ m^2/g$ was used in this study. According to the manufacture, this powder contained 1 wt % oxygen, 220 ppm carbon, and trace amounts of iron, calcium, and silicon. 1 mol % of a Y_2O_3 powder (average particle size: 1.6 μm, specific surface area: $8.4\ m^2/g$, supplied by Shin–Etsu Chemical) as a sintering aid was added to the raw AlN powder. These powders were mixed in ethanol for 12 h using a plastic bottle mill with Al_2O_3 balls. After drying, the mixed powder was pressed into circular cylinders (14 mm in diameter and 8 mm in height) and rectangular cylinders (8×6 mm and 40 mm in height) using stainless steel dies, and cold isostatically pressed (CIPed) under 400 MPa for 60s. The CIPed bodies were wrapped in carbon foils and then sintered in a tungsten resistance furnace at temperatures of 1773, 1873, 1973, 2073 and 2173 K for 1 h in a 0.1 MPa nitrogen gas atmosphere. The CIPed samples were also sintered at 2173 K for 2, 3 and 5 h in the same atmosphere. The heating rate was $15\ K\ min^{-1}$ for all the cases.

The bulk density was measured by a displacement method in water. Disks of 10 mm diameter and 3.5 mm thickness were prepared for thermal coefficient measurements by a laser flash method (Shinku–Riko, TC–3000 H) at room temperature. The thermal conductivity (κ_m) was calculated from the experimental values of thermal diffusivity (α), specific heat capacity (C) and density (D) as:

$$\kappa_m = \alpha C D \quad (1)$$

The equipment and detailed procedures for thermal coefficient measurements have been described elsewhere [13]. The oxygen contents of the sintered AlN were analysed by a radioactive analysis method. The crystalline phases of the sintered bodies were determined by X-ray diffraction.

The trapped gases in the sintered AlN were evaluated by a mass spectrometer attached to an ultra-high

0022–2461/91 $03.00 + .12

vacuum chamber (pressure: 10^{-8} Pa or less) of an Auger electron spectrometer (AES). Notched specimens (3 × 3 mm and 20 mm in length) were fractured in the ultra-high vacuum chamber and the gases released from the fractured samples were detected. The equipments and detailed procedures of mass spectrometer analysis used in this work have been reported elsewhere [14, 15].

The fractured surfaces were observed by a scanning electron micrograph (SEM). The grain sizes of sintered bodies were measured from SEM photographs of fractured surfaces.

3. Results

Fig. 1 shows the relationship between the relative density of sintered AlN and the sintering temperature. The AlN specimen was fully densified at 2173 K for 1 h.

The thermal conductivities of specimens are shown in Fig. 2a and b. These values were calibrated by the total porosity of the sintered AlN using the following equation [16].

$$[\kappa_d = \kappa_m/(1 - P)] \quad (2)$$

where κ_d and κ_m are, respectively, the thermal conductivity of a densified body and an empirically measured one and P is the total porosity of the specimen. The sintered AlN exhibits an increase in thermal conductivity by a factor of about six, from 30 to 180 $Wm^{-1}K^{-1}$, when the sintering temperature is increased from 1773 to 2173 K (Fig. 2a). Also the thermal conductivity of AlN ceramics sintered at 2173 K increased with increasing sintering periods.

Fig. 3 shows the oxygen content of sintered AlN. Oxygen contents decreased linearly from 2.8 to 0.6 wt % when the sintering temperature was increased from 1773 to 2173 K for 1 h, as shown in Fig. 3a. Also, the oxygen content decreased from 0.6 to 0.1 wt % when the sintering period was increased from 1 to 5 h at a sintering temperature of 2173 K, as plotted in Fig. 3b.

The oxygen content in the sintered AlN influences the thermal conductivity. Fig. 4 shows the relationship between the thermal conductivity and the oxygen content of AlN specimens obtained in this work. The results reported by Slack [2], Sakai [3], Kuramoto [4], Horiguchi [11] and Kurokawa [17] were also plotted. The AlN thermal conductivity was increased by decreasing the oxygen content of sintered body. In the present work, the thermal conductivity increased from 30 to 220 $Wm^{-1}K^{-1}$ with decreasing oxygen content from 2.8 to 0.1 wt %.

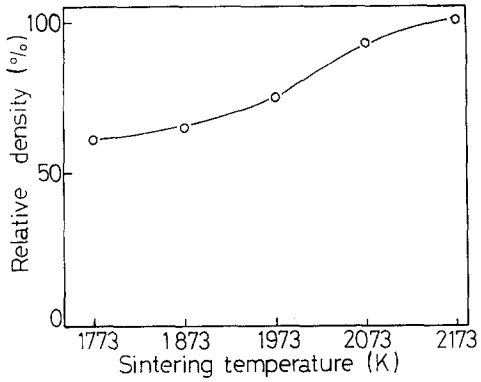

Figure 1 The relative density of sintered AlN plotted against sintering temperature sintered for 1 h. The theoretical density of sintered AlN is estimated as 3260 kg m^{-3}

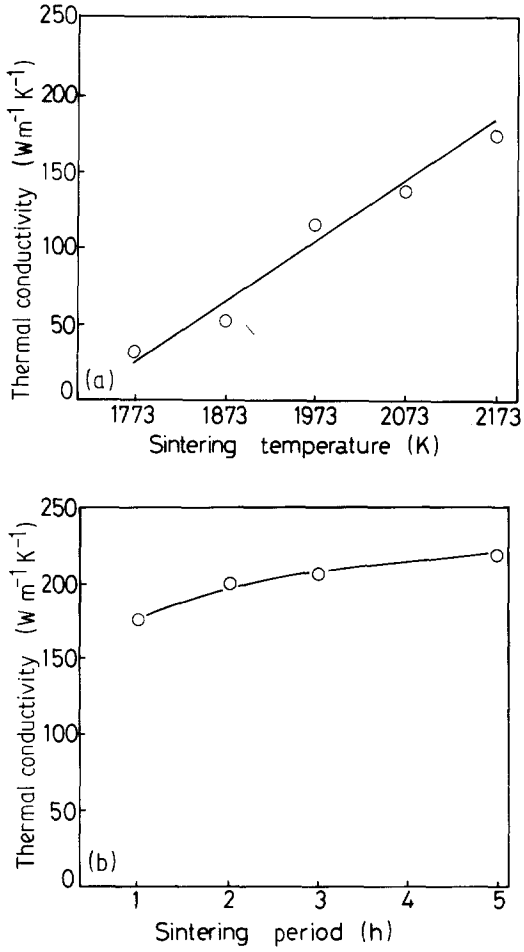

Figure 2 Thermal conductivity plotted against (a) sintering temperature sintered for 1 h and (b) sintering periods sintered at 2173 K.

Fig. 5 shows the X-ray diffraction spectra used to analyse which crystalline phases were formed in the sintered AlN. In the samples sintered at lower temperatures $Al_2Y_4O_9$ ($2Y_2O_3 \cdot Al_2O_3$) is stable, but YN becomes more stable for those sintered at higher temperatures. Left in air at room temperature for about 48 h, grey YN powder formed on the surface of the AlN ceramics sintered at 2073 K for 1 h and at 2173 K for 1, 2, 3 and 5 h. Yagi *et al.* investigated the change of grain boundary phases during AlN sintering and found a large amount of YN phase on the surface of sintered AlN. Also they reported the difference of grain boundary phases on the surface and inside of the sintered AlN [18]. In the present experiment Y_2O_3 was stable instead of YN at about 1 mm depth from the surface of AlN specimens at 2073 K and 2173 K for 1 h.

Fig. 6a, b and c shows the mass spectra of the trapped gases released from the fractured samples. Each sample was fractured 10 s after starting the measurement. The abscissa is analysis time. In the

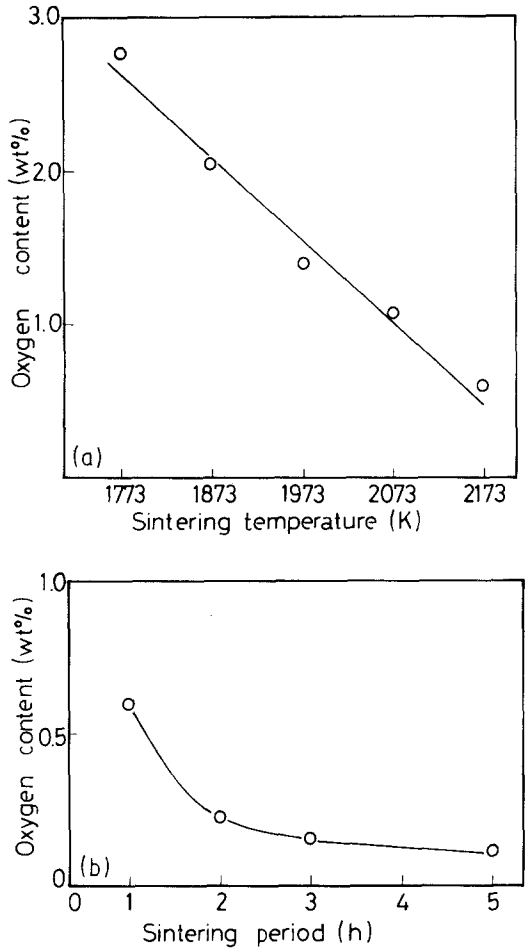

Figure 3 Oxygen content of sintered AlN plotted against (a) sintering temperature sintered for 1 h and (b) sintering periods sintered at 2173 K.

present work, the gases of CO and CO_2 were detected from the fractured AlN.

Fig. 7a, b, and c shows SEM micrographs of the fractured AlN surfaces, which were broken in an ultra-high vacuum chamber for mass spectrometer analysis. Almost all of them were fractured along grain boundaries. It is, therefore, considered that the CO and CO_2 gases exist in grain boundaries of sintered AlN. Also AlN grain size increased with increasing sintering temperature and sintering period duration, as shown in Fig. 8. The grain size of AlN specimens obtained was about 1–10 μm.

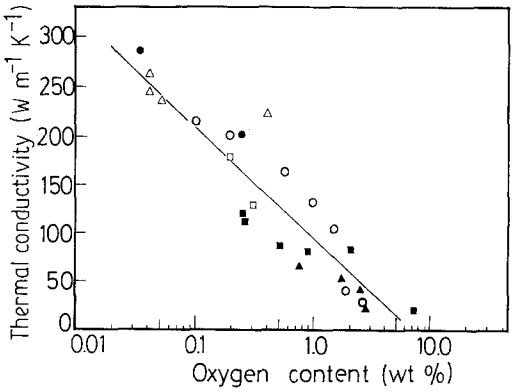

Figure 4 Thermal conductivity plotted against oxygen content of sintered AlN. (○) This work; (●) [2]; (▲) [3]; (■) [4, 6]; (□) [5, 17]; (△) [11].

4. Discussion

The AlN sintering in a reducing nitrogen atmosphere has been reported to be a useful method to obtain sintered bodies with high thermal conductivities [10–12]. The possible reducing reactions are [12, 19];

$$Al_2O_3 + N_2 + 3C \leftrightharpoons 2AlN + 3CO \quad (3)$$

$$Al_2Y_4O_9 + N_2 + 3C \leftrightharpoons 2AlN + 2Y_2O_3 + 3CO \quad (4)$$

and

$$Y_2O_3 + N_2 + 3C \leftrightharpoons 2YN + 3CO \quad (5)$$

The stability of products for the reactions shown in Equations 3 and 5 during AlN sintering have been explained using the standard free energy change of the reactions by the authors elsewhere [19]. However, the evidences of reactions shown in Equations 3, 4 and 5 were not confirmed. In this work, these reactions

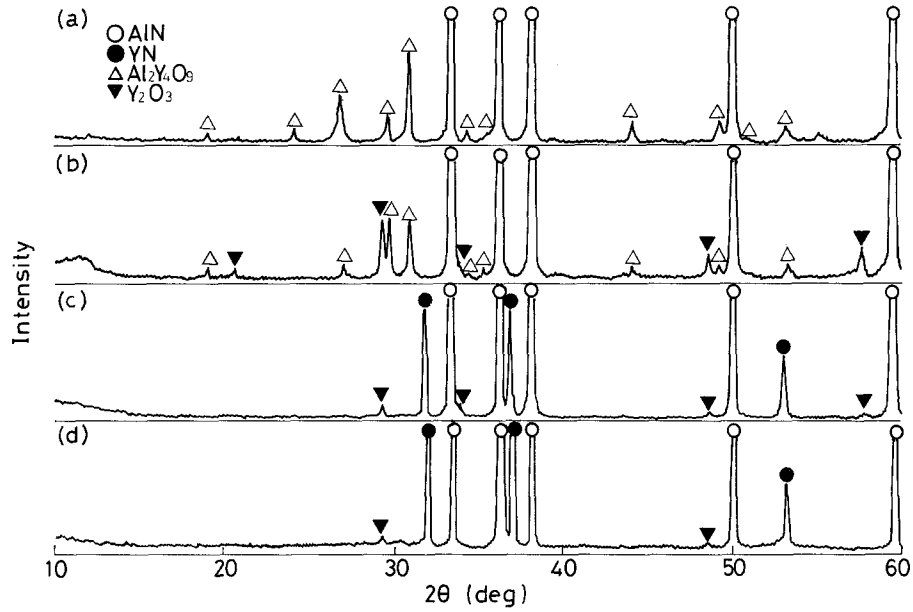

Figure 5 The crystalline phases of the surface of AlN ceramics sintered for 1 h at sintering temperatures of (a) 1873 K, (b) 1973 K, (c) 2073 K and (d) 2173 K.

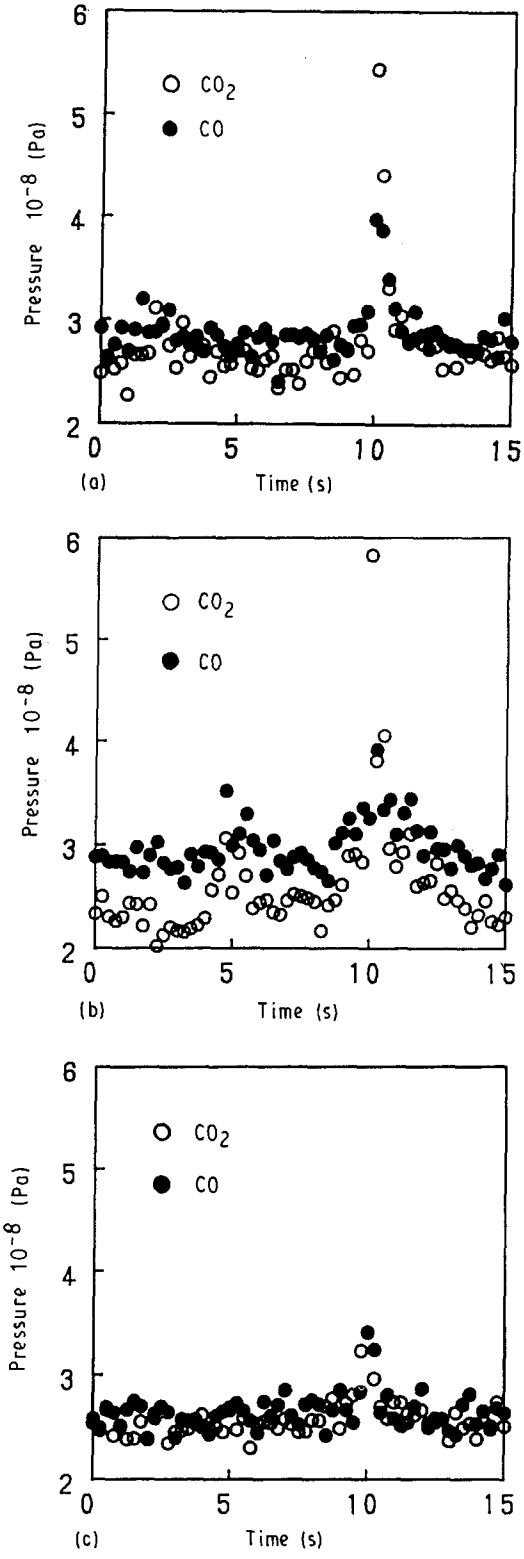

Figure 6 Mass spectra in the fractured surface of specimens sintered for 1 h at sintering temperatures of (a) 1973 K, (b) 2073 K and (c) 2173 K. Each sample was fractured in the ultra-high vacuum chamber (pressure, 10^{-8} Pa or less).

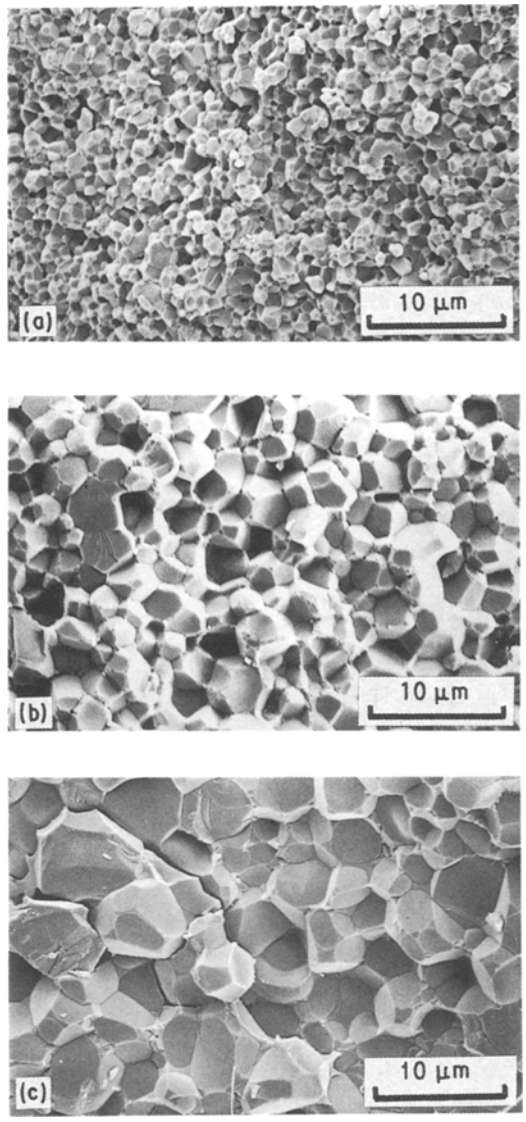

Figure 7 SEM micrographs of the fractured surface for AlN specimens sintered for 1 h at sintering temperatures of (a) 1973 K, (b) 2073 K and (c) 2173 K. The bars indicate 10 μm.

were clarified by examining the oxygen contents, the grain boundary phases of the sintered AlN and the trapped gas in the sintered bodies.

Equation 3 is a production reaction to obtain raw AlN powder by carbo-nitriding Al_2O_3 [20]. It is considered that oxygen atoms exist as Al_2O_3 and/or AlON on the particle surface of AlN. Sakai *et al.* reported that an amorphous oxide film on the AlN particles had a depth of around 400–1200 nm [3]. In the present experiment, the amount of Al_2O_3 containing the raw AlN powder used was about 2 wt %, assuming that all the oxygen detected forms Al_2O_3. From thermodynamic consideration, this reaction occurs at higher temperatures than 1973 K and under lower oxygen partial pressure than 10^{-11} Pa [19]. Therefore the reaction shown in Equation 3 could take place in the present work. Because sintering temperature was high enough, and oxygen partial pressure was about 10^{-11} Pa which was governed by the carbon foils.

Although the $Al_2Y_4O_9$ phase in the sintered AlN is stable at a sintering temperature of 1873 K for 1 h, the Y_2O_3 phase becomes more stable at a sintering temperature of 1973 K for 1 h. The CO gas was detected from the fractured surface of samples sintered at 1973 K. Therefore the reaction shown in Equation 4 is estimated from the present results. Yagi *et al.* pointed out that the $Al_2Y_4O_9$ as a grain boundary phase decomposed into Y_2O_3 and Al_2O_3, which migrated towards the surface of the sintered body and were nitrided on the surface to form a surface layer of YN and AlN [18]. In the present sintering, the $Al_2Y_4O_9$

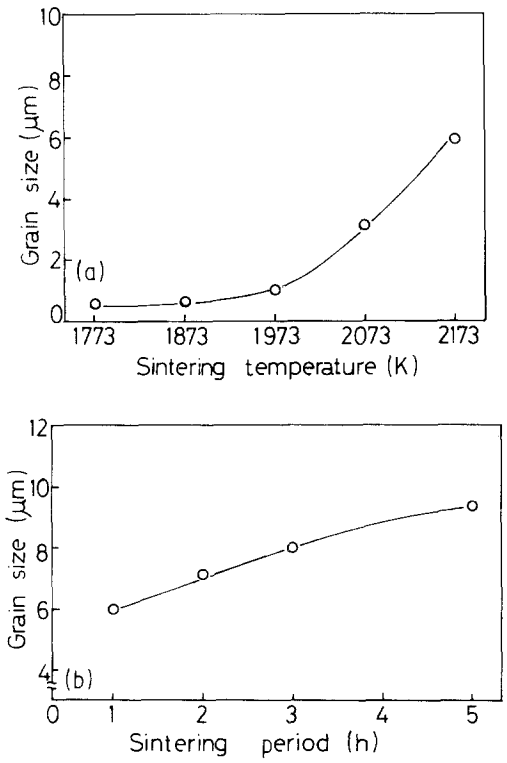

Figure 8 Change of grain size of sintered AlN plotted against (a) sintering temperature sintered for 1 h and (b) sintering periods at 2173 K.

grain boundary phase must be decomposed into Y_2O_3 and Al_2O_3 to form a Y_2O_3 grain boundary phase. Therefore the Al_2O_3 phase must be produced during sintering but was not found by X-ray diffraction analysis. The reason why Al_2O_3 was not found might be due to the quick reaction velocity for the carbo-nitriding Al_2O_3 or the small amount of Al_2O_3.

At a sintering temperature of 1973 K, Y_2O_3 and small $Al_2Y_4O_9$ phases were detected on the surface of the AlN bodies. However, the YN phase becomes more stable for the samples sintered at higher temperatures (2073 and 2173 K). Also, CO gas was detected from both specimens sintered at temperatures of 2073 K and 2173 K for 1 h. Considering the presence of YN and CO gas, the reaction shown in Equation 5 is estimated. On the basis of thermodynamic consideration, the authors reported that this reaction occurs at higher temperatures than 2223 K and with a lower oxygen partial pressure than 10^{-9} Pa [19].

In the mass spectrometer analysis, CO_2 gas was detected as well as CO gas. The possible reactions are as follows instead of Equations 3, 4 and 5

$$Al_2O_3 + N_2 + 3CO \leftrightharpoons 2AlN + 3CO_2 \quad (3a)$$

$$Al_2Y_4O_9 + N_2 + 3CO \leftrightharpoons 2AlN + 2Y_2O_3 + 3CO_2 \quad (4a)$$

and

$$Y_2O_3 + N_2 + 3CO \leftrightharpoons 2YN + 3CO_2 \quad (5a)$$

The CO gas of these reactions is the gas which formed around the specimens during sintering because of oxygen impurity in the raw AlN powder and the fact that carbon was used. Therefore the oxygen partial pressure during sintering was assumed to be along a line corresponding to $2C + O_2 \leftrightharpoons 2CO$ [19]. Consequently, CO_2 gas formed by the reactions shown in Equations 3a, 4a and 5a. CO_2 gas was detected in the mass spectrometer analysis and was reduced to CO because of the presence of carbon foils ($CO_2 + C \leftrightharpoons 2CO$).

The use of these chemical reactions to decrease oxygen content during AlN sintering with Y_2O_3 additive in a reducing nitrogen atmosphere with carbon were confirmed in the present work. The reactions shown in Equations 3a, 4a and 5a during AlN sintering proceed with increasing sintering temperature and period duration and resulted in AlN of high thermal conductivity.

5. Conclusions

The chemical reactions to increase thermal conductivity by decreasing oxygen contents during the sintering of AlN with an Y_2O_3 additive in a reducing nitrogen atmosphere were investigated. It was shown that:

1. Reactions to decrease the oxygen content in the sintered AlN were confirmed as follows: (a) $Al_2O_3 + N_2 + 3CO \leftrightharpoons 2AlN + 3CO_2$; (b) $Al_2Y_4O_9 + N_2 + 3CO \leftrightharpoons 2AlN + 2Y_2O_3 + 3CO_2$; and (c) $Y_2O_3 + N_2 + 3CO \leftrightharpoons 2YN + 3CO_2$. Some of the CO_2 gas reduced to CO gas because of the presence of the carbon foils ($CO_2 + C \leftrightharpoons 2CO$)
2. The oxygen contents of sintered AlN decreased with increasing sintering temperature and sintering period duration and AlN thermal conductivity increased as a result.
3. The oxygen atoms in the sintered AlN were released mainly as CO and CO_2 gases.
4. The $Al_2Y_4O_9$ grain boundary phase of sintered AlN transformed to Y_2O_3 and YN as the sintering temperature increased.

References

1. K. KOMEYA and H. INOUE, *J. Mater. Sci.* **4** (1969) 1045.
2. G. A. SLACK, *J. Phys. Chem. Solids.* **34** (1973) 321.
3. T. SAKAI, M. KURIYAMA, T. INUKAI and T. KIJIMA, *J. Ceram. Soc. Jpn* **86** (1978) 30.
4. N. KURAMOTO, H. TANIGUCHI, Y. NUMATA and I. ASO, *ibid.* **93** (1985) 517.
5. Y. KUROKAWA, K. UTSUMI and H. TAKAMIZAWA in Proceedings of Symposium on the Basic Science of Ceramics, Ceramics Society of Japan, Sendai (Japan 1986) p. 174.
6. N. KURAMOTO and H. TANIGUCI, *J. Mater. Sci. Lett.* **3** (1984) 471.
7. K. SHINOZAKI, K. ANZAI, T. TAKANO, A. TSUGE and K. KOMEYA in Proceedings of Symposium on the Basic Science of Ceramics. Ceramics Society of Japan, Kyoto (Japan 1984) p. 43.
8. K. KOMEYA, H. OHTA, K. SHINOZAKI, H. INOUE and A. TSUGE, *ibid.* p. 44.
9. K. SHINOZAKI and A. TSUGE, *Bull. Ceram. Soc. Jpn.* **21** (1986) 1130.
10. M. KASORI, A. HORIGUCHI, F. UENO and A. TSUGE, in Proceedings of the Annual Meeting of the Ceramics Society of Japan, Nagoya, Japan, (1987) p. 967.
11. A. HORIGUCHI, M. KASORI, F. UENO and A. TSUGE, *ibid.* p. 969.
12. M. OKAMOTO, H. ARAKAWA, M. OOHASHI and S. OGIHARA, *J. Ceram. Soc. Jpn* **97** (1989) 1478.
13. K. WATARI, Y. SEKI and K. ISHIZAKI, *ibid.* **97** (1989) 174, or *J. Ceram. Soc. Jpn., Inter. Edn* **97** (1989) 170.

14. M. KAWAMOTO, C. ISHIZAKI and K. ISHIZAKI, *J. Mater. Sci. Lett.* **10** (1991) 279.
15. M. KAWAMOTO and K. ISHIZAKI, *J. Mater. Sci. Lett.* **7** (1989) 1193.
16. W. D. KINGERY, H. K. BOWEN and D. R. UHLMAN, in "Introduction to Ceramics", (John Wiley, New York, 1960) p. 504.
17. Y. KUROKAWA, K. UTSUMI and H. TAKAMIZAWA, *J. Amer. Ceram. Soc.* **71** (1988) 588.
18. T. YAGI, K. SHINOZAKI, N. MIZUTANI, M. KATO and Y. SAWADA, *J. Ceram. Soc. Jpn* **97** (1989) 1372.
19. K. ISHIZAKI and K. WATARI, *J. Phys. Chem. Solids* **50** (1989) 1009.
20. M. UDA, S. OHNO and H. OKUYAMA, *J. Ceram. Soc. Jpn* **95** (1987) 76.

Received 15 January
and accepted 6 November 1990